Available online at www.sciencedirect.com
ScienceDirect
International Journal of Mass Spectrometry 266 (2007) 15–24
International Journal of Mass Spectrometry
www.elsevier.com/locate/ijms

Mass spectrometer analysis of plasma containing easily dissociated species: Absolute concentrations of the main free radicals $Si(CH_3)_{1,2,3}$, and $H_2Si(CH_3)$ produced in a microwave discharge sustained in an Ar–$Si(CH_3)_4$ gas mixture

J.L. Jauberteau *, I. Jauberteau, J. Aubreton

SPCTS-UMR 6638 CNRS, Faculté des Sciences, 123 av A. Thomas, 87060 Limoges, France

Received 16 April 2007; received in revised form 7 June 2007; accepted 11 June 2007
Available online 16 June 2007

Abstract

This paper deals with the experimental methods developed using mass spectrometer to analyse the gas composition in plasma containing molecular species with a low dissociation threshold. These methods are developed to study mainly the case of a plasma produced in an Ar–$Si(CH_3)_4$ gas mixture. The $Si(CH_3)_4$ tetramethylsilane molecule is interesting because it is easily dissociated within the plasma. However, this molecule and the radicals produced in the plasma are also easily dissociated into the mass spectrometer ionization chamber. Thus, special investigation methods, taking into account the various dissociation processes of the different species, is required to correct the mass spectrometer signal intensity. Classical first correction methods are used, and concern the transmission factor depending on parameters like the m/z ratio and the emission electron current intensity into the mass spectrometer ionization chamber. We also develop a new method with the aim of correcting the dissociative ionization part of the molecular precursor involved in the signal intensity. This method is first tested in the simpler case of an Ar–CH_4 mixture containing plasma, then is applied to plasma sustained in an Ar–$Si(CH_3)_4$ gas mixture. We discuss the influence of the different dissociative ionization processes to the signal intensity corresponding to the main $Si(CH_3)_{1,2,3}$ and $H_2Si(CH_3)$ radicals observed at $m/z = 73$, 58, 45, and 43, at electron energy lower than 30 eV. We show that in that case, the signal intensity of these $Si(CH_3)_{1,2,3}^+$, $H_2Si(CH_3)^+$ ions is mainly due to the direct ionization of the parent radicals.

Keywords: Microwave plasma; Tetramethylsilane; Mass spectrometer; Radical density; Plasma discharge

1. Introduction

Plasma discharges are widely used as a basic technology for microelectronic devices, surface treatment, conversion chemistry, and full of other applications [1–6]. However, because of the large amount of radicals produced therein, the analysis of plasmas containing heavy molecular species is often difficult. Mass spectrometer is a promising tool to analyse the composition of such plasma. It gives information about ions and neutral species contained in complex gas mixtures, and it is generally suitable to determine relative or absolute concentrations of species. However, because of plasma discharge working conditions, mass spectrometer analysis requires specifics adaptations. The purpose of this work is to determine the concentrations of the main radicals, which are produced in the plasma. So, it is necessary to study the effect of various parameters on the signal intensity, like the emission current intensity in the ionization chamber, or the effect of the m/z ratio. We also study the contribution of the various dissociative ionization processes, occurring in the ionization chamber of the mass spectrometer. All the signal corrections are discussed in the following parts.

2. Experimental setup

The experimental setup is shown in Fig. 1. It consists of a microwave discharge (SAIREM generator working at 2.45 GHz) produced in a quartz tube (internal diameter 16 mm and external diameter 19 mm). The precursor is injected in the reactor

* Corresponding author.
E-mail address: jean-louis.jauberteau@unilim.fr (J.L. Jauberteau).

1387-3806/$ – see front matter © 2007 Elsevier B.V. All rights reserved.
doi:10.1016/j.ijms.2007.06.009

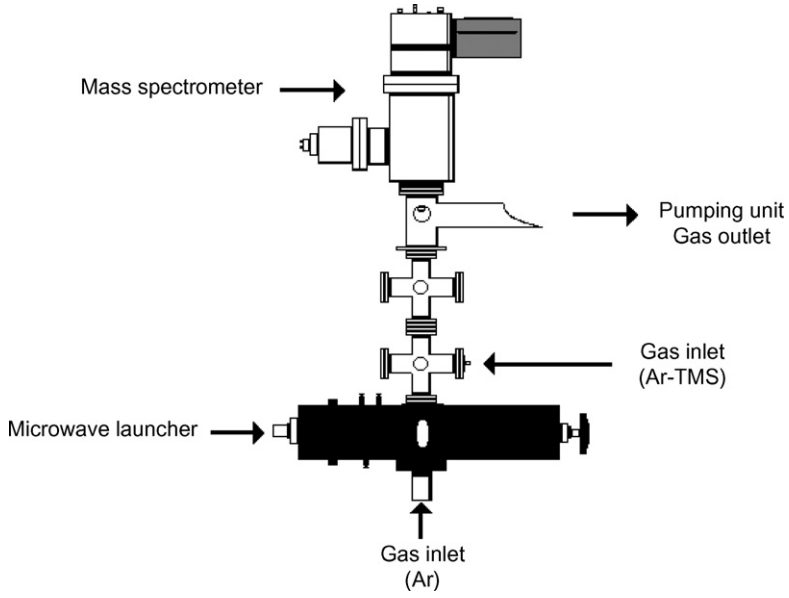

Fig. 1. Experimental setup.

mixed to argon. According to the experimental conditions, the precursor inflow is upstream or downstream of the discharge. Fig. 1 shows the case where the precursor is injected downstream. In order to keep a constant wall temperature, the quartz tube is refreshed by means of pulsed air. The total pressure in the discharge tube is held constant and is ranging from 10 to 100 Pa using a roots blower pumps (70–700 m^3/h), that allows a constant gas flow velocity, ranging from 10 to 30 m/s, in the stainless tube with inner diameter of 50 mm located above the discharge and collecting species produced into the discharge. The mass spectrometer (QMG 421 Balzers) is fixed above this stainless steel tube at an adjustable distance above the discharge. A grounded stainless steel tube placed above the discharge is used to trap all remaining ions coming from the discharge up to the mass spectrometer analyser placed downstream. The efficiency of the ion trap is tested using an electrostatic probe placed above the ion trap, and measuring the residual ion currents. Before each experiment, the reactor is heated and pumped at 10^{-4} Pa and maintained at this pressure for several hours by means of a molecular pump in order to clean the reactor wall. Because the quadrupole cannot operate at pressure higher than 10^{-3} Pa, a two-stage differential pumping unit is required. It consists of two pumping groups with a molecular pump and a dry primary pump, one of these groups is used for the vacuum in the quadrupole and the other is connected at an intermediate chamber between the reactor and the quadrupole. This special setup is shown in Fig. 2. In the first stage (pump 2 in the figure) the molecular pump has a vacuum speed in N_2 equal to 210 l/s

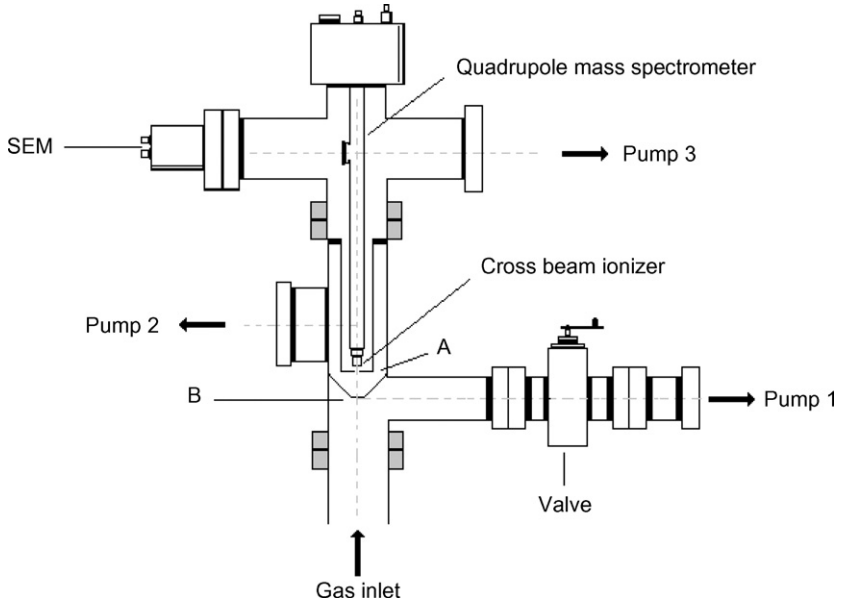

Fig. 2. The mass spectrometer device.

and in the second stage (pump 3) the molecular pump is smaller and the vacuum speed is 56 l/s. During the analysis the pressure is equal to 10^{-4} Pa in the second stage where the quadrupole is located and ranges between 10^{-2} and 10^{-3} Pa in the first stage. The extraction hole located between the analyser and the reactor (B in the figure) has a diameter equal to 100 μm and the second hole located between the two stages (A in the figure) is 500 μm. The distance between the two holes is equal to 6.5 cm, to keep the mean free path larger than the distance between the two extraction holes fixed at the entrance of each stage. So, particles cannot recombine into this intermediate chamber. The first sample hole (part B) is located in the stainless steel tube of 50 mm diameter few centimetres below the cross point between this first tube axis and the gas outlet tube axis connected to the roots blower pump (pump 1 in the figure). In this device, the gas flow remains undisturbed and can be considered as a plug flow.

The ionization chamber consists of an electron cross beam apparatus placed 5 mm above the 500 μm diameter hole just before the quadrupole (QMA 400 Balzers). The experimental error on the energy values is equal to 0.2 eV. Before each experiment, the filaments of the electron cross beam apparatus are heated to clean the surface using a current intensity ranges between 0 and 3 A for about 1 h.

3. Comments on the mass spectrometer signal intensity measured

3.1. The transmission factor

The mass spectrometer signal intensity I_i measured for species i, when only the direct ionization process occurs can be written [7]

$$I_i = T\sigma_{(i^+/i)}(\varepsilon_e)n_i = A\sigma_{(i^+/i)}(\varepsilon_e)i_e n_i \quad (1)$$

where T ($T = Ai_e$) is the transmission factor, which depends on the effective electron beam current intensity (i_e) crossing the ionization chamber, on the m/z ratio, on the sensitivity of the quadrupole, and on the vacuum conductivity of the gas through the orifice in the extractor. $\sigma_{(i^+/i)}(\varepsilon_e)$ is the ionization cross-section at the electron energy ε_e and, n_i is the concentration of species i.

As shown in Fig. 3a, the transmission factor increases with increasing electron energy and decreases with increasing m/z. At a low electron energy (<30 eV) it strongly increases with increasing electron energy then for larger m/z values, it increases slowly with increasing electron energy up to an asymptotic value corresponding to an electron energy larger than 70 eV.

Fig. 3b shows the change of the transmission factor ($T = Ai_e$) versus the ratio m/z, measurements are performed at 20 Pa at 70 and 30 eV, respectively. In collisionless conditions ($\lambda_i \gg \lambda_D$), the sampled ion flux is proportional to $(m_i)^{-1/2}$ [8], so at low m/z values (<15), the transmission factor quickly decreases with increasing m/z. It decreases slowly with increasing m/z for larger m/z values. At 70 eV, for $m/z = 2$, the transmission factor is equal to 1.9×10^{-3}, it is equal to 6.3×10^{-4} for $m/z = 16$ and to 3.4×10^{-4} for $m/z = 32$. For the heavy species ($m/z > 30$), the transmission factor is quite constant with increasing m/z and can be supposed constant for $m/z > 30$.

The value of the transmission factor depends also of the electron energy because of the change in the electron current intensity crossing the ionization chamber. This one increases with electron energy increasing. Within the ionization chamber, the effective electron current intensity (i_e) emitted from the filament and crossing the chamber depends on the electron energy given by the positive acceleration voltage U_e applied between the filament and the anode. The dependence of i_e with the extraction voltage is described by the Langmuir's law [9–11]

$$i_e = PU_e^{3/2} \quad (2)$$

P is a value depending on the geometry of the ionization chamber. The dependence of i_e with U_e is observed until i_e is equal to the saturation value, given by the thermoionic current intensity value calculated using the Richardson–Dushman equation [10,11].

The emission electron current is usually easily stabilized. However, a too large current intensity value producing a too high filament temperature could produce a strong evaporation and a change in the filament area, and a new thermoionic current value.

The relative electron current intensity crossing the ionization chamber can be deduced from the mass spectrometer signal intensity measured for species i using the relation, deduced from Eq. (1),

$$\frac{i_e}{i_{eo}} = \frac{I_i}{I_{io}} \frac{\sigma(\varepsilon_{eo})}{\sigma(\varepsilon_e)} \quad (3)$$

where $\sigma(\varepsilon_e)$ is the ionization cross-section at the electron energy ε_e.

Fig. 4a and b shows the change of the relative emission electron current intensity versus electron energy. Measurements are performed for Ar($m/z = 40$) and N_2($m/z = 28$) at pressure ranges from 6×10^{-3} to 55 Pa. The ionization cross-section values are given in [12]. In both cases the results are compared to the theoretical values calculated using the Langmuir's law, Eq. (2). The relative emission electron current intensity crossing the ionization chamber increases from 0.2 to 1 with the electron energy increasing from 20 to 35 eV. The emission electron current rises up, when a positive voltage is applied in front of the filament.

The difference observed Fig. 4a and b, between experimental values and calculated values using the Langmuir's law, Eq. (2), is probably due to the divergence of the electron beam before the entrance slit of the ionization chamber. One part of the electron beam is striking the electron slits of the ionization chamber. It is the "stray electron current" [13]. The other part corresponds to the electron beam crossing the ionization chamber efficient to ionize the neutral sampled species. It is the "trap electron current". It can be shown that the part of the trap electron current increases with electron energy increasing. The difference observed between the measured and the calculated electron current values when the pressure is changing, is probably due to the change of the gas flow conductivity through the sample hole.

These first results show that a good knowledge of the transmission factor and consequently of the emitted electron

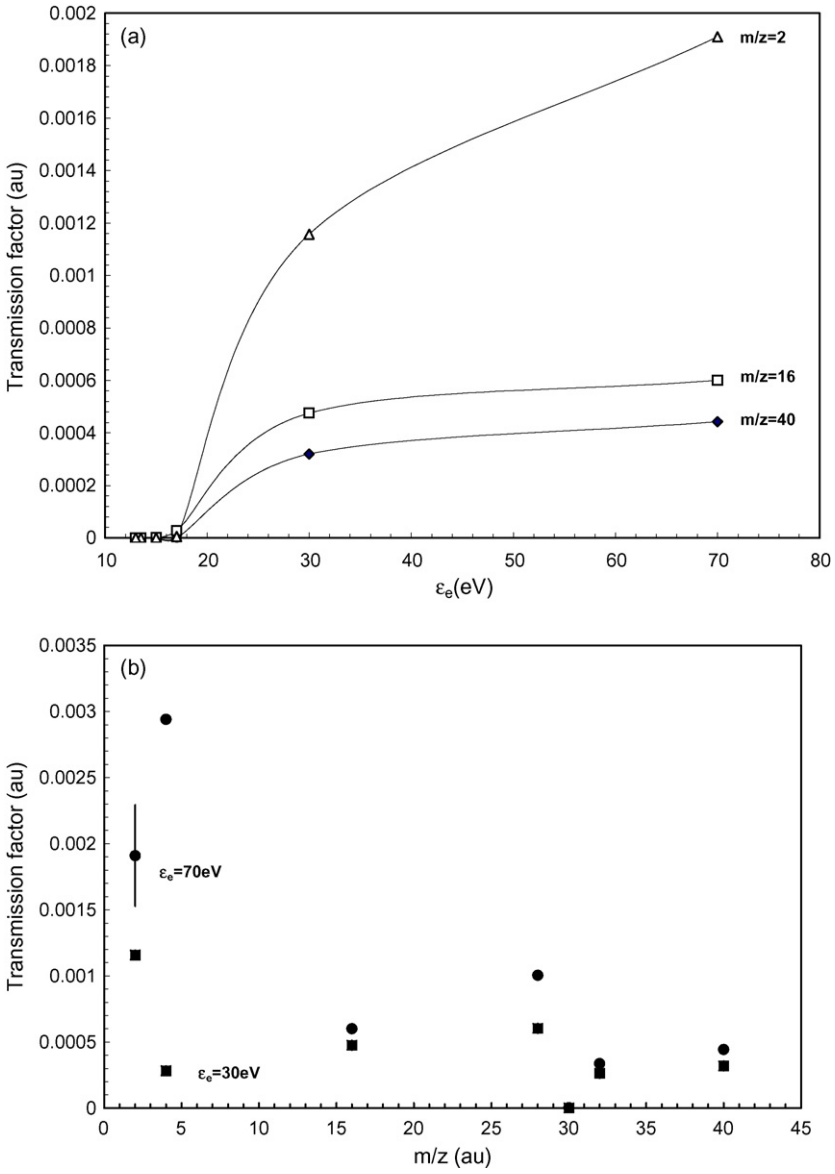

Fig. 3. (a) The transmission factor vs. the electron energy, measurements are performed for various *m*/*z* ratios. The pressure is kept constant equal to 66.6 Pa. (b) The transmission factor vs. the *m*/*z* ratio, measurements are performed at 66.6 Pa at two different electron energies 70 and 30 eV.

current intensity crossing the ionization chamber is necessary to compare measurements performed under various experimental conditions. As previously related, the transmission factor also depends on the sample hole gas flow conductivity, which depends on the pressure within the reactor. So, corrections are applied to compare measurements performed at pressures corresponding to different gas flow through the sample hole.

3.2. Effect of dissociative ionization processes on the mass spectrometer signal intensity

For plasma containing easily dissociated molecules, the signal intensity measured for species *i* is the sum of the part due to the direct ionization of species *i*, and of the parts due to the various dissociative ionization processes of larger species *j* producing ions i^+ [14–16]. The mass spectrometer signal intensity is the sum of all these different contributions, and can be written,

$$I_i = I(i^+/i) + \sum\nolimits_j I(i^+/j) = T_i\sigma_{(i^+/i)}(\varepsilon_e)n_i + T_i\sum\nolimits_j(\sigma_{(i^+/j)}(\varepsilon_e)n_j) \quad (4)$$

where $\sigma_{(i^+/i)}(\varepsilon_e)$ is the ionization cross-section due to the direct ionization of species *i* and $\sigma_{(i^+/j)}(\varepsilon_e)$ is the dissociative ionization cross-section of species *j* producing ions i^+. If the measurements are performed within the discharge, we must also take into account the part of the signal intensity, which is due to the ion i^+ produced within the discharge.

So, in the case of plasma producing a lot of neutral species *j*, with a low dissociative ionization threshold, it is very difficult and often not possible to determine the real part of the signal intensity measured for i^+ corresponding to the direct ionization of the species *i* only.

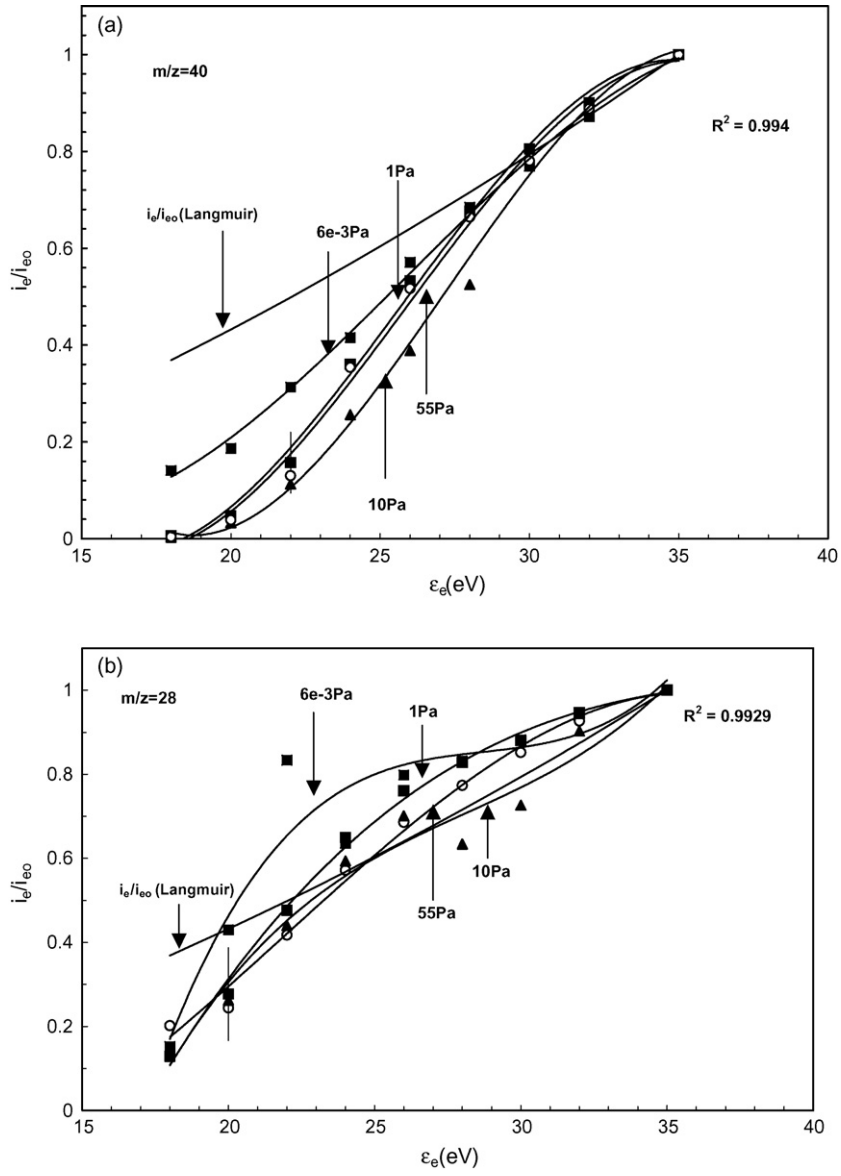

Fig. 4. (a) The relative electron current in the ionization chamber vs. the electron energy at different pressure. Measurements are performed for $m/z = 40$. (b) The relative electron current at 20 Pa vs. the ionization source current (filament current) at two electron energies 20 and 30 eV. Measurements are performed for $m/z = 28$.

In former works [7,17,18], authors have developed a method to separate the part of the signal due to the direct ionization from the part due to the dissociative ionization. They applied this method named the threshold ionization technique to the case of CH_2 and CH_3 radicals, produced in an Ar–CH_4 discharge and to SiH_3 radicals produced in an Ar–SiH_4 discharge. This method is based on the difference between the appearance potential of the dissociative ionization and the direct ionization potential of the free radical. In the case of CH_3^+, the part due to the direct ionization of CH_3 can be estimated at electron energy ranging from 9.8 to 14.3 eV, because the dissociative ionization potential corresponding to $CH_4 + e \rightarrow CH_3^+ + 2e + H$ is observed at 14.3 eV and the direct ionization potential of the free radical corresponding to $CH_3 + e \rightarrow CH_3^+ + 2e$ is observed at 9.8 eV. However, at low electron energy the mass spectrometer signal intensity measured is low and strongly disturbed. So, it is difficult to determine accurate radical concentration values from the direct ionization signal measured. Our method consists of measuring the current at larger electron energy. That leads to a less disturbed signal.

The previous idea is well illustrated by the effect of the dissociative ionization processes. Let us consider the simple case of an Ar–CH_4 plasma. CH_4 molecule is smaller than $Si(CH_3)_4$ and produces less radicals. We define the R factor equal to the relative contribution of the dissociative ionization of the initial precursor CH_4 to the signal intensity measured for species i.

$$R = \frac{I_i - I_i(\text{corr})}{I_i} = \frac{I_i(\text{diss})}{I_i} \tag{5}$$

where I_i is the signal intensity measured and I_i(corr) is the signal intensity after correction of the part due to the contribution of the dissociative ionization I_i(diss) of CH_4 initial precursor. That

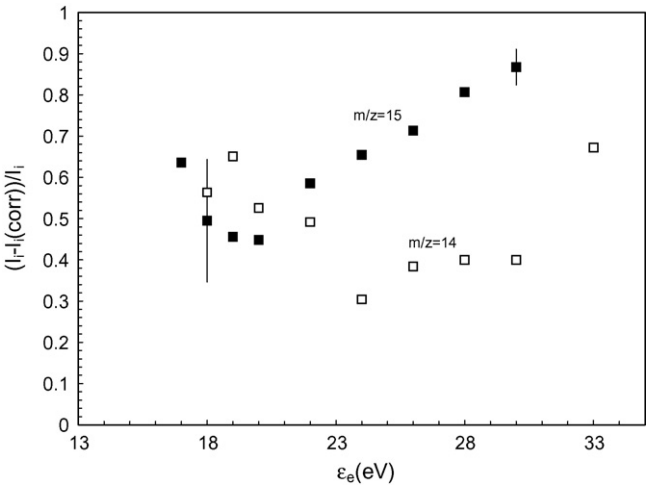

Fig. 5. The R factor vs. the electron energy for $m/z = 14$ and 15. The methane injection is realised downstream of the argon discharge. The total pressure is 0.2 mBar and the methane pressure is 0.05 mBar.

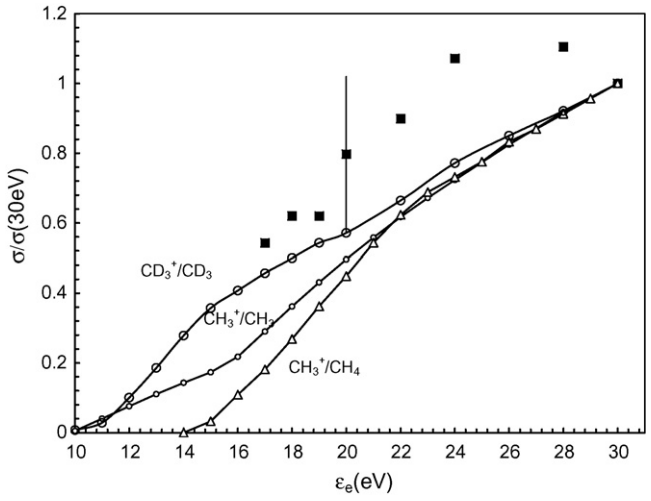

Fig. 6. σ/σ (30 eV) measured for $m/z = 15$ vs. ε_e. Comparison with the direct ionization processes (empty circle) given by NIST and Tarnovsky et al. [19,20] and the dissociative ionization process (empty pyramid) given by Chatham et al. [21].

can be approximated using the equation [15]:

$$I_i(\text{diss}) = \frac{I_i(\text{off}) I_{\text{pr}}(\text{on})}{I_{\text{pr}}(\text{off})} \tag{6}$$

where $I_{i(\text{off})}$, I_{pr}(on) and I_{pr}(off) are the signal intensity due to species i when the discharge is off, the signal intensity measured for the precursor when the discharge is on and when it is off, respectively. I_{pr} is $I_{(m/z=16)}$ and $I_{(m/z=88)}$ in the case of CH_4 or $Si(CH_3)_4$ precursor, respectively.

Fig. 5 displays the variation of R factor versus electron energy, calculated for the two ions CH_3^+ and CH_2^+. The measurements have been performed above a microwave discharge working at 15 W when the precursor is injected downstream of an argon discharge. So a large amount of radicals are not dissociated. It can be observed, that the R factor increases with electron energy increasing. The relative contribution of the dissociative ionization of CH_4 is equal to 80 and 40% for CH_3 and CH_2 respectively at electron energy equal to 30 eV.

Figs. 6 and 7 display the relative ionization cross-section $\sigma(\varepsilon_e)/\sigma(30\,\text{eV})$ versus the electron energy measured for CH_3^+ and CH_2^+. Measurements are performed downstream of an Ar–CH_4 microwave discharge. The relative ionization cross-section is calculated after correction, suppressing to the signal intensity measured the part due to the dissociative ionization of CH_4, using the equation [16],

$$\frac{\sigma(\varepsilon_e)}{\sigma(\varepsilon_{eo})} = \frac{I_i(\varepsilon_e)}{I_i(\varepsilon_{eo})} \frac{i_e(\varepsilon_{eo})}{i_e(\varepsilon_e)} \tag{7}$$

Here $\varepsilon_{e0} = 30$ eV.

Figs. 6 and 7 also compare experimental results to the values displays in the literature for the direct ionization of radical CH_3, CD_3 or CH_2 [19,20], and the dissociative ionization of CH_3 (here CD_3) and CH_4 producing CH_2^+, and CH_3^+ [20,21]. It can be seen that for CH_3^+, the relative ionization values are close to the values given in the literature for the direct ionization of CH_3. However, in the case of CH_2^+, the relative ionization is similar to the values given in the literature in the case of the dissociative ionization of CH_3 producing CH_2^+. The ionization threshold value measured (about 16 eV) is above the value given for the direct ionization of CH_2 (10.5 eV [19]) and close to the value given by Tarnovsky et al. [20] for the dissociative ionization of CH_3 (#15 eV) producing CH_2^+. These results show that in the case of the ion CH_3^+, the signal intensity is probably mainly due to the direct ionization of CH_3 and in the case of CH_2^+, the signal intensity is largely due to the dissociative ionization of CH_3 and probably also partly due to the direct ionization of CH_2.

In the case of a plasma discharge containing Ar–$Si(CH_3)_4$ gas mixture, the tetramethylsilane molecule has a ionization threshold ranges from 9 to 10 eV [22] and the ionization proceed simultaneously to the direct ionization and to the dissocia-

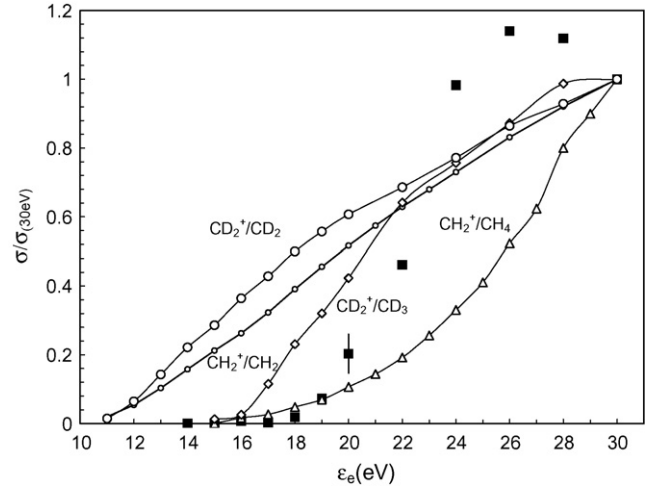

Fig. 7. σ/σ (30 eV) measured for $m/z = 14$ vs. ε_e. Comparison with the direct ionization processes (empty circle) given by NIST and Tarnovsky et al. [19,20] and the dissociative ionization process (empty pyramid for CH_2^+/CH_4) given by Chatham et al. [21] and (empty diamond for CD_2^+/CD_3) given by Tarnovsky et al. [20].

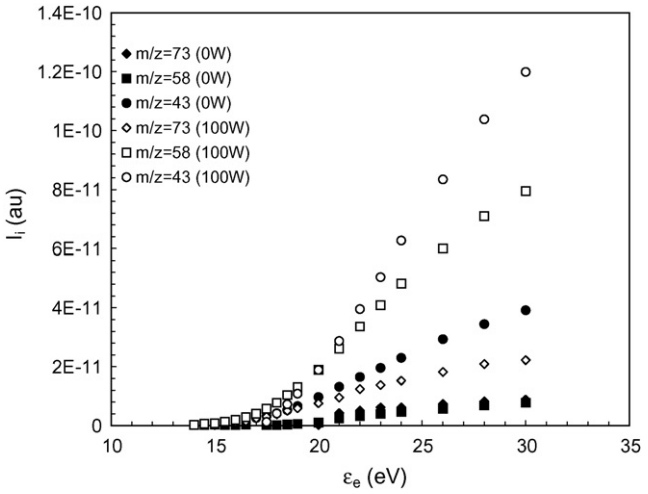

Fig. 8. The mass spectrometer signal intensity measured for $m/z = 73$, 58 and 43 vs. the electron energy. The measurements are performed when the discharge is off (0 W) and on (100 W).

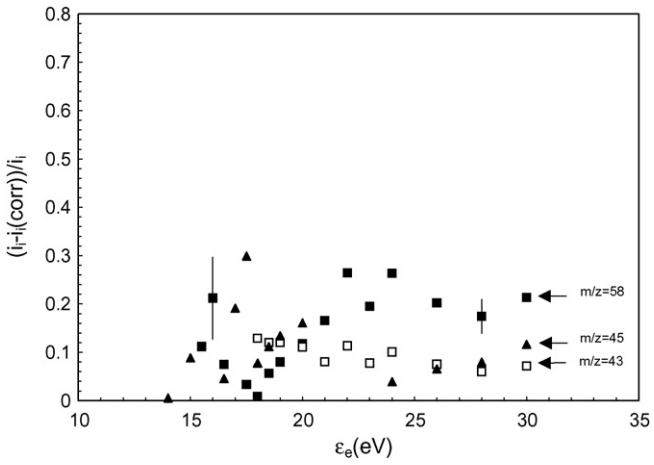

Fig. 9. The R factor vs. ε_e, for $m/z = 58$ (full square), 45 (full pyramid), and 43 (empty square). The tetramethylsilane is injected upstream of the argon discharge working at 25 W. The total pressure is 26.6 Pa and the tetramethylsilane pressure is 6.5 Pa.

tive ionization producing $Si(CH_3)_4^+$, $Si(CH_3)_3^+$, $Si(CH_3)_2^+$ and $Si(CH_3)^+$ and other ions. So it is difficult to separate the various ionization mechanisms because they are nearly simultaneously produced. Moreover, other radicals $Si_xC_yH_z$ and ions $Si_xC_yH_z^+$ can also be produced in the discharge. The signal intensity measured in the case of different species corresponding to $m/z = 73$, 58 and 43 versus electron energy when the discharge is off (0 W) and on (at 100 W) are shown in Fig. 8. In this case, the tetramethylsilane is injected upstream of the discharge in argon. The total pressure is equal to 26 Pa and the tetramethylsilane pressure is equal to 6 Pa. All the different ions are detected even at low electron energy when the discharge off. At 30 eV the signal measured for $m/z = 73$ when the discharge is off is equal to 40% of the signal measured at 100 W, it is 10% for $m/z = 58$ and 33% for $m/z = 43$. So, it is necessary to separate the part of the signal intensity due to the direct ionization of species i producing ions i^+ from the part due to the dissociative ionization of other species larger than species i, and producing also i^+ ions. About the contribution of the remaining tetramethylsilane, the contribution of the dissociative ionization to the signal measured for an ion i is relatively easy to determine, it can be deduced from the signal measured when the discharge is off, using Eq. (6).

Because the Si–C and C–H binding energies are equal to 355 and 421 kJ/mol respectively [23], the dissociative ionization process of $Si_xC_yH_z$ species is expected to proceed mainly via Si–C bond breaking rather than C–H bond breaking and the main ionization processes are,

$$R\text{–}CH_3 + e \rightarrow R^+ + CH_3 + 2e \quad (1a)$$

or

$$R\text{–}CH_3 + e \rightarrow R + CH_3^+ + 2e. \quad (1b)$$

Considering $Si(CH_3)_{1,2,3}$ and $H_2Si(CH_3)$ main radicals produced in the discharge and corresponding to $m/z = 73$, 58, 43 and 45 respectively, the part of the dissociative ionization processes in the signal intensity is due to the dissociative ionization of the tetramethylsilane ($m/z = 88$, the precursor) in the case of $m/z = 73$, to the dissociative ionization of $m/z = 88$ and $m/z = 73$ for $m/z = 58$ and to the dissociative ionization of $m/z = 88$, 73 and 58 for $m/z = 43$. In the case of $m/z = 45$, $H_2Si(CH_3)$ species are produced by the desorbed species from the reactor wall [24], probably $H_2Si(CH_3)_2$ or $HSi(CH_3)_2$ and consequently the dissociative processes contributing to the signal intensity measured are not the same that for the other species.

As previously seen in the case of CH_3^+, and CH_2^+, we report the R factor measured for all these species versus the electron energy in Figs. 9–11. The measurements are performed when the tetramethylsilane is injected upstream of the argon discharge at different power 25, 50 and 100 W, respectively. It can be seen that for electron energy upper than 17–18 eV, the R factor remains roughly unchanged when the electron energy is increasing. At lower electron energy the R factor roughly decreases with increasing electron energy. However, because of the large error on measurements performed at low electron energy, this behaviour is doubtful. Whatever the power is (between 25 and

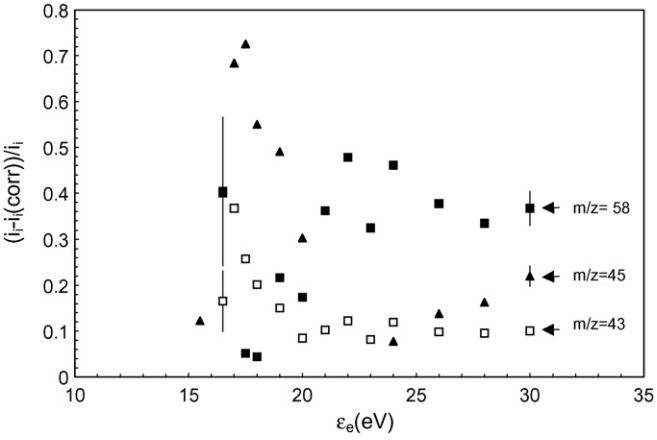

Fig. 10. The R factor vs. ε_e, for $m/z = 58$ (full square), 45 (full pyramid), and 43 (empty square). The tetramethylsilane is injected upstream of the argon discharge working at 50 W. The total pressure is 26.6 Pa and the tetramethylsilane pressure is 6.5 Pa.

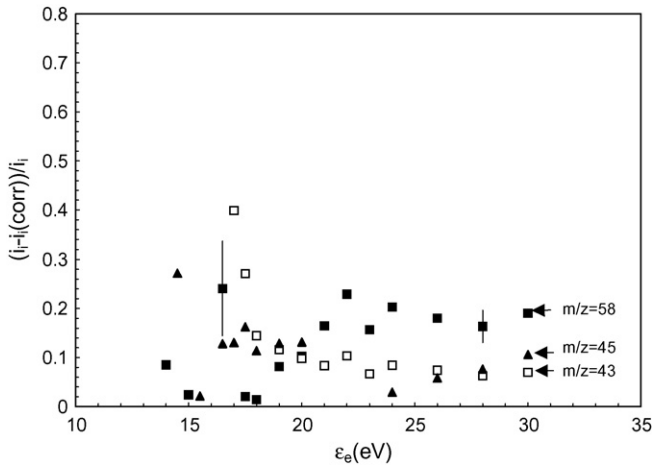

Fig. 11. The R factor vs. ε_e, for $m/z = 58$ (full square), 45 (full pyramid), and 43 (empty square). The tetramethylsilane is injected upstream of the argon discharge working at 100 W. The total pressure is 26.6 Pa and the tetramethylsilane pressure is 6.5 Pa.

100 W), the R factor for $\varepsilon_e > 18$ eV is low and ranges from 10 to 20% for $m/z = 43$ and 45. It is larger and ranges from 10 to 40% for $m/z = 58$. These R factor values are low and observed when the precursor is injected upstream the discharge i.e., when the precursor is strongly dissociated. However, in the particular case of $m/z = 73$, not reported in the figures, the R factor is close to 1. This value can be explained assuming that $m/z = 73$ is not produced when Ar–$Si(CH_3)_4$ is injected upstream of the discharge because of the strong dissociation. In this case, the signal intensity value for $m/z = 73$ after correction using Eq. (6) is low and nearly equal to 0, so R is close to 1.

When Ar–$Si(CH_3)_4$ is injected downstream of the discharge working at 20 W (Fig. 12), the dissociation is low and $m/z = 73$ species are mainly produced. The R factor is now close to one for the other species $m/z = 58$, 45 and 43, because of the low signal intensity value after correction using Eq. (6). However, for $m/z = 73$, the R factor is quite stable at electron energy larger

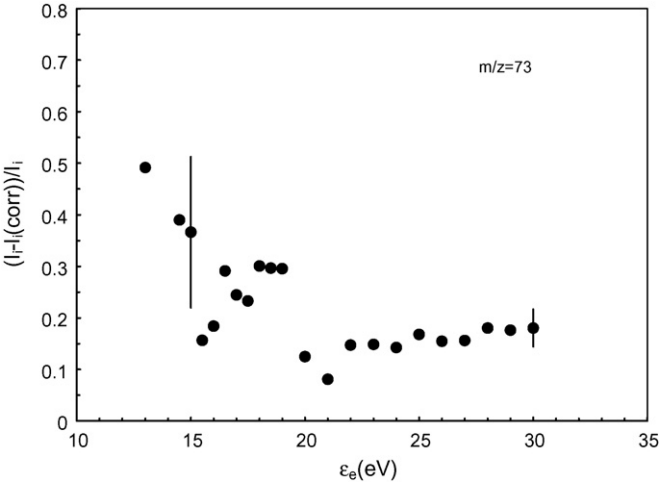

Fig. 12. The R factor vs. ε_e, for $m/z = 73$. The tetramethylsilane is injected downstream of the argon discharge working at 20 W. The total pressure is 40 Pa and the tetramethylsilane pressure is 13.3 Pa.

than 20 eV and is close to 15%, as it is shown in Fig. 12. As previously observed at low electron energies (<15 eV), the R factor values are systematically larger and less stable than for high electron energies >20 eV. This is due to the large error performed on the signal intensity value.

After correction of the signal intensity, when the dissociative ionization part of $Si(CH_3)_4$ is removed, the signal intensity corresponding to $m/z = 73$ is only due to the direct ionization of the $Si(CH_3)_3$ radical. However, in the case of the other species ($m/z = 58$, 45 and 43), dissociative ionization processes due to radicals or species desorbed by the reactor walls in the case of $m/z = 45$ [24], can contribute to increase the signal intensity corresponding to these ions. As previously done in the case of an Ar–CH_4 microwave discharge, we have measured the relative ionization cross-section determined for $m/z = 15$ versus electron energy, in the case of an Ar–$Si(CH_3)_4$ gas mixture and compare these results to the data given in the literature and corresponding to different ionization processes. Fig. 13 shows the change of $\sigma(\varepsilon_e)/\sigma(30\,\text{eV})$ versus the electron energy ranges from 10 to 30 eV. Results are compared with data given in the literature for the direct ionization of CH_3 or CD_3 [19,20], and with the dissociative ionization of C_2H_6 [21] and $Si(CH_3)_4$ [25] producing CH_3^+. Measurements are performed when the gas mixture containing the precursor is injected upstream of the argon discharge at 100 and 25 W. The figure shows two behaviours for the ionization processes. At low electron energy (roughly lower than 20 eV), the relative ionization cross-section increases slowly with increasing electron energy. At these electron energies, CH_3^+ is probably mainly due to the direct ionization of the CH_3 radical, as it was previously reported in a former work [24].

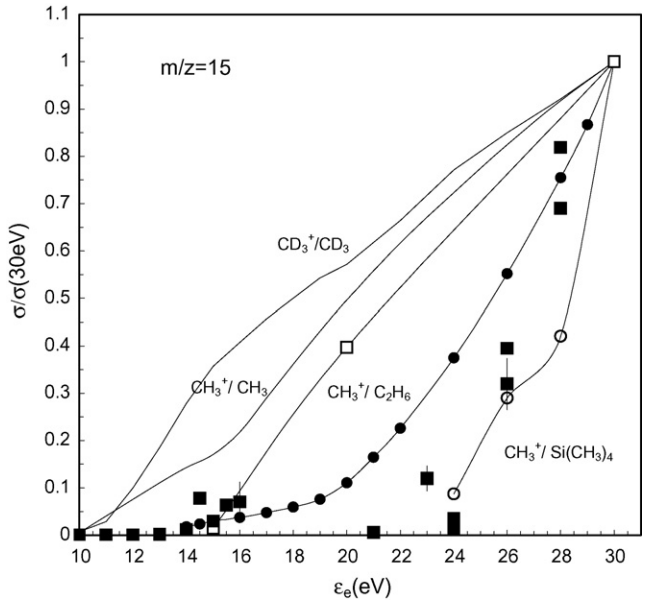

Fig. 13. σ/σ (30 eV) measured for $m/z = 15$ vs. ε_e. Measurements are performed when the tetramethylsilane is injected upstream of the discharge working at 100 W (full square), and 25 W (full circle). Comparison is realised with value given by NIST (full thin line for CH_3^+/CH_3) [19], Tarnovsky et al (dotted thin line for CD_3^+/CD_3) [20], for the direct ionization and Chatham et al. (empty square for CH_3^+/C_2H_6) [21], Basner et al (empty circle for $CH_3^+/Si(CH_3)_4$) [25], for the dissociative ionization processes.

At larger electron energy, others ionization processes producing CH_3^+ occur. Because of the correction done using Eq. (6), they are not due to the tetramethylsilane molecule but to the main radicals (SiC_xH_y) produced in the discharge.

4. Absolute concentration of the main radicals $Si(CH_3)_{3,2,1}$ and $H_2Si(CH_3)$

We have measured the concentration of the main radical produced in the plasma. $Si(CH_3)_{3,2,1}$ radicals result mainly of Si–C bonds breaking. We have also measured the absolute concentration of $H_2Si(CH_3)$ resulting of desorbed species from the reactor wall. After correction of the influence of the dissociative ionization of the remaining tetramethylsilane using Eq. (6), we assume in a first approximation that the signal intensity measured for $m/z = 73$, 58, 45 and 43, is mainly due to the direct ionization of radicals $Si(CH_3)_{1,2,3}$ and of $H_2Si(CH_3)$. Thus, using Eq. (1), it is possible to determine the relative concentrations of these radicals. Figs. 14–16 displays the absolute concentration of $Si(CH_3)_{3,2,1}$ and $H_2Si(CH_3)$ versus the tetramethylsilane partial pressure injected downstream of the discharge, measurements have been performed at 100, 150 and 200 W, respectively and at an argon pressure equal to 66 Pa. The absolute concentrations for species i is determined comparing the signal measured for the species to the signal measured when the discharge is off, which corresponds only to the dissociative ionization processes of $Si(CH_3)_4$, producing ion j^+. So, the concentration is given by,

$$n_i = n_{\mathrm{tms}} I_{(i^+/i)}(\varepsilon_e)/I_{(j^+/\mathrm{tms})}(\varepsilon_e)\,\sigma_{(j^+/\mathrm{tms})}(\varepsilon_e)/\sigma_{(i^+/i)}(\varepsilon_e). \quad (8)$$

In this equation, n_i, n_{tms} are the concentration of the species i and of the tetramethylsilane injected within the reactor, respectively. $I_{(i^+/i)}(\varepsilon_e)$ and $I_{(j^+/\mathrm{tms})}(\varepsilon_e)$ are the signal intensity measured when the discharge is on for the species i, and when the discharge is off for species j. $\sigma_{(j^+/\mathrm{tms})}(\varepsilon_e)$ and $\sigma_{(i^+/i)}(\varepsilon_e)$ are the dissociative ionization cross-section of the tetramethylsilane producing j^+ [25] and the direct ionization cross-section of i producing i^+ [16]. j^+ can be i^+ or any other ions produced in the ionization chamber and used as reference.

It can be seen in Figs. 14–16 that the main radicals produced is $Si(CH_3)$, then $Si(CH_3)_2$ and $Si(CH_3)_3$. At 100 W the concentration ratio is roughly 1/10/100 for $m/z = 73$, 58 and 43, respectively. The radical concentration increases with power increasing at least until 200 W. Fig. 16 also displays the concentration measured for $m/z = 45$ at 200 W. The concentration of this species is equal to that of $m/z = 73$. At low power, $m/z = 45$ species are difficult to observe because the concentration is much

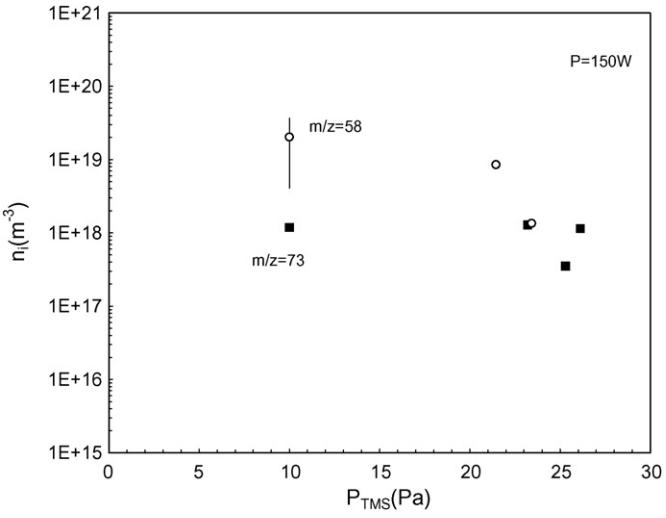

Fig. 15. The absolute concentration measured for radicals $m/z = 73$ (full square), 58 (empty circle) vs. the tetramethylsilane pressure injected downstream of the argon discharge working at 150 W. The argon pressure is fixed equal to 66 Pa and the electron energy in the ionization chamber is 18 eV.

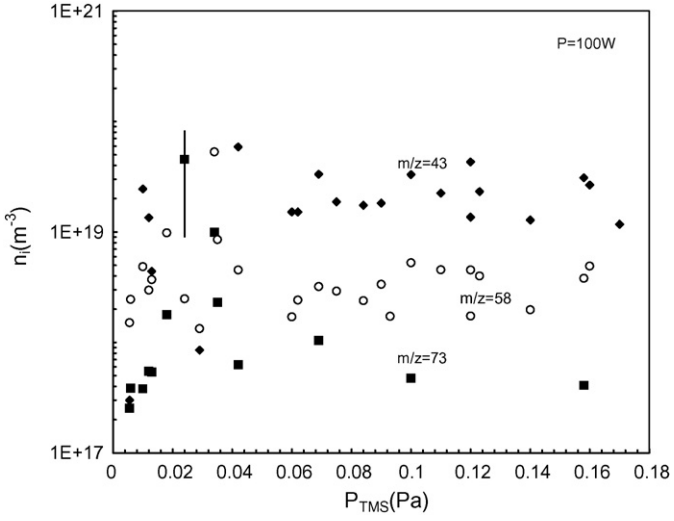

Fig. 14. The absolute concentration measured for radicals $m/z = 73$ (full square), 58 (empty circle), and 43 (full diamond) vs. the tetramethylsilane pressure injected downstream of the argon discharge working at 100 W. The argon pressure is fixed equal to 66 Pa and the electron energy in the ionization chamber is 30 eV.

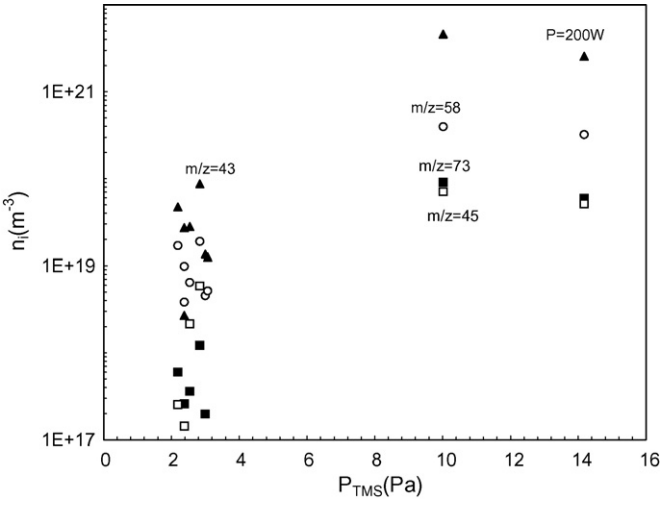

Fig. 16. The absolute concentration measured for radicals $m/z = 73$ (full square), 58 (empty circle), 45 (empty square) and 43 (full diamond) vs. the tetramethylsilane pressure injected downstream of the argon discharge working at 200 W. The argon pressure is fixed equal to 66 Pa and the elctron energy in the ionization chamber is 16 eV.

lower due to the decrease of desorbed species from the wall [24]. It can be seen that the concentration of the species first increases with increasing tetramethylsilane partial pressure then slowly decreases for large partial pressure values. The maximum is shifted to larger partial pressure value with increasing power. It is equal to 0.1–0.2 Pa at 100 W, 5–7 Pa at 150 W and 8–10 Pa at 200 W.

As in the case of CH_3^+, the ionization processes are expected to results mainly of the direct ionization of the radical, at low electron energy, $\varepsilon_e < 20$ eV (see Fig. 13). In Figs. 15 and 16, measurements have been perform at electron energy of 16 and 18 eV, and the results show that the absolute concentration of $Si(CH_3)_3$ is one order of magnitude lower than the concentration of $Si(CH_3)_2$, and two order of magnitude lower than the $Si(CH_3)$ concentration. From these results, it appears that because of the low concentration of $m/z = 73$ compared to $m/z = 58$ and 43, the dissociative ionization process of $Si(CH_3)_3$ is expected to contribute weakly to the signal intensity measured for $m/z = 58$ and 43. So, as expected the signal intensity corresponding to $m/z = 58$ is probably mainly due to the direct ionization of $Si(CH_3)_2$ only. The same comments can be done concerning the signal measured for $m/z = 43$. Because of the low concentration of $Si(CH_3)_2$ compared to the concentration of $Si(CH_3)$, the contribution of the dissociative ionization of $Si(CH_3)_2$ to the signal measured for $m/z = 43$ is probably low.

Thus, the calculation of the absolute concentration of the different species confirms our previous assumption: the contribution of dissociative ionization processes of $Si(CH_3)_3$ radical to the signal intensity measured for $m/z = 58$ and 43, and of $Si(CH_3)_2$ to the signal intensity measured for $m/z = 43$ can be in a first approximation neglected, and the signal intensity can be mainly ascribed to the direct ionization of radicals $Si(CH_3)_3$, $Si(CH_3)_2$, and $Si(CH_3)$, respectively. At least at electron energy lower than 30 eV.

5. Conclusion

This paper deals with the experimental methods developed using mass spectrometer to analyse the gas composition in plasma containing molecular species with a low dissociation threshold. First we give the main corrections used on the signal intensity. These corrections take into account the effect of the electron current in the ionization chamber, the effect of the m/z ratio and of the pressure. Moreover, because of the large contribution of the dissociative ionization processes, it is necessary to make other corrections on the signal intensity measured. We give a method, which can be used in order to suppress the dissociative ionization due to the parent molecules in the signal measured for the different species. Then, we discuss the contribution of the other dissociative ionization processes to the signal corresponding to the main radicals in plasma sustained both in $Ar–CH_4$ and $Ar–Si(CH_3)_4$ gas mixture. In the case of an $Ar–Si(CH_3)_4$ gas mixture, we calculate the absolute concentration of these radicals and we prove that because of the low relative $Si(CH_3)_3$ concentration compared to $Si(CH_3)_2$, and of $Si(CH_3)_2$ compared to $Si(CH_3)$, the contribution of the dissociative ionization of these radicals to the signal measured for each $Si(CH_3)_{1,2,3}^+$ ions is probably low and so the signal intensity results mainly of the direct ionization of the parent radicals. This result confirms our assumption concerning the low dissociative ionization contribution to the signal intensity measured at low electron energy (<30 eV).

References

[1] A. Oumghar, J.C. Legrand, A.M. Diamy, N. Turillon, Plasma Chem. Plasma Process. 15 (1995) 87.
[2] I. Jauberteau, J.L. Jauberteau, M. Cahoreau, J. Aubreton, in: J.M. Menon (Ed.), Trends in Vacuum Science & Technology, vol. 4, Research Trends, Trivandrum, India, 2001, p. 77.
[3] M.E. Fraser, D.A. Fee, R.S. Sheinson, Plasma Chem. Plasma Process. 5 (1985) 63.
[4] I. Jauberteau, M. Cahoreau, J.L. Jauberteau, J. Aubreton, J. Phys. D: Appl. Phys. 38 (2005) 3654.
[5] A.M. Wrobel, G. Czeremuskin, H. Szymanowski, J. Kowalski, Plasma Chem. Plasma Process. 10 (1990) 277.
[6] R.A.B. Zijlmans, O. Gabriel, S. Welzel, F. Hempel, J. Röpcke, R. Engeln, D.C. Schram, Plasma Sources Sci. Technol. 15 (2006) 564.
[7] H. Toyoda, H. Kujima, H. Sugai, Appl. Phys. Lett. 54 (1989) 1502.
[8] M.J. Vasile, H.F. Dylla, in: O. Auciello, D.L. Flamm (Eds.), Plasma Diagnostics, vol. 1, Academic Press Inc., 1989.
[9] T. Durakiewicz, S. Halas, Int. J. Mass Spectrom. 177 (1998) 155.
[10] T.D. Märk, E. Hille, J. Chem. Phys. 69 (1978) 2492.
[11] I. Langmuir, Phys. Rev. 21 (1913) 450.
[12] D. Rapp, P. Englander-Golden, J. Chem. Phys. 43 (1965) 1464.
[13] K. Stephan, H. Helm, T.D. Märk, J. Chem. Phys. 73 (1980) 3763.
[14] J.L. Jauberteau, I. Jauberteau, J. Aubreton, J. Phys. D: Appl. Phys. 35 (2002) 665.
[15] J.L. Jauberteau, J. Aubreton, I. Jauberteau, Int. J. Mass Spectrom. 189 (1999) 63.
[16] J.L. Jauberteau, I. Jauberteau, J. Aubreton, J. Appl. Phys. 99 (2006) 1249081.
[17] (a) H. Kojima, H. Toyoda, H. Sugai, Appl. Phys. Lett. 55 (1989) 1292; (b) H. Toyoda, H. Kojima, H. Sugai, Appl. Phys. Lett. 54 (1989) 1507.
[18] R. Robertson, D. Hils, H. Chatham, A. Gallagher, Appl. Phys. Lett. 43 (1983) 544.
[19] National Institue of Standards and Technology (NIST). http://physics.nist.gov/PhysRefData/Ionization.html.
[20] V. Tarnovsky, A. Levin, H. Deutsch, K. Becker, J. Phys. B: At. Mol. Phys. 29 (1996) 139.
[21] H. Chatham, D. Hils, R. Robertson, A. Gallagher, J. Chem. Phys. 81 (1984) 1770.
[22] H.M. Rosenstock, K. Draxl, B.W. Steiner, J.T. Herron, J. Chem. Phys. Data 6 (1977).
[23] A.M. Wrobel, Plasma Chem. Plasma Process. 7 (1987) 429.
[24] J.L. Jauberteau, J. Aubreton, I. Jauberteau, Int. J. Mass Spectrom. 228 (2003) 49.
[25] R. Basner, R. Foest, M. Schmidt, F. Sigeneger, P. Kurunczi, K. Becker, H. Deutsch, Int. J. Mass Spectrom. 153 (1996) 65.